Hindawi Publishing Corporation
Journal of Nanomaterials
Volume 2014, Article ID 714010, 7 pages
http://dx.doi.org/10.1155/2014/714010

Research Article

Nanoporous Activated Carbon Derived from Rice Husk for High Performance Supercapacitor

Huaxing Xu, Biao Gao, Hao Cao, Xueyang Chen, Ling Yu, Kai Wu, Lan Sun, Xiang Peng, and Jijiang Fu

The State Key Laboratory of Refractories and Metallurgy, School of Materials and Metallurgy, Wuhan University of Science and Technology, Wuhan 430081, China

Correspondence should be addressed to Biao Gao; gaobiao@wust.edu.cn and Jijiang Fu; fujijiang@wust.edu.cn

Received 4 November 2014; Revised 1 December 2014; Accepted 2 December 2014; Published 29 December 2014

Academic Editor: Chunyi Zhi

Nanoporous activated carbon material was produced from the waste rice husks (RHs) by precarbonizing RHs and activating with KOH. The morphology, structure, and specific surface area were investigated. The nanoporous carbon has the average pore size of 2.2 nm and high specific area of 2523.4 $m^2 g^{-1}$. The specific capacitance of the nanoporous carbon is calculated to be 250 $F g^{-1}$ at the current density of 1 $A g^{-1}$ and remains 80% for 198 $F g^{-1}$ at the current density of 20 $A g^{-1}$. The nanoporous carbon electrode exhibits long-term cycle life and could keep stable capacitance till 10,000 cycles. The consistently high specific capacitance, rate capacity, and long-term cycle life ability makes it a potential candidate as electrode material for supercapacitor.

1. Introduction

The increasing market for portable electronic devices (PED) and hybrid vehicles (HV) leads to demand for high performance electrochemical capacitors [1]. Currently commercially available electrochemical supercapacitors (SC) are of electrical double-layer capacitors (EDLCs) for their long-term cycle life (more than 100,000 cycles) and high power density [2]. Due to the high specific surface area, good conductivity, and low cost, porous carbon materials are widely used as electrode materials for EDLCs [3]. Transformation of low cost renewable biomass into porous carbon provides a green, low cost, and facile method for carbon electrode of EDLCs, which is of significant research and commercial interest. Up to date, some natural biomass materials such as cassava peel waste, chicken eggshell, seed shell, rubber wood sawdust, wood, peanut kernel, and sugar have been exploited as precursors for the production of porous carbons for SC and lithium ion secondary batteries electrodes [4–7].

Rice husks (RHs), as a common form of agricultural biomass, are the major by-product in the rice milling industry. The global rice production is about 600 million tons per year and more than 100 million tons of RHs, as the RHs make up about 20% of the rice paddy weight. This huge amount of waste by-product is an environmental nuisance; hence, developing uses for this waste resource is in accord with the global paradigm shift towards sustainable development. The major contents of the RHs are cellulose (38%), hemicellulose (18%), lignin (22%), and inorganic silica. The overall carbon element content in RHs is more than 37% by weight [8]. One promising application of RHs utilization is to the generation of sustainable carbon materials for SCs. Very recently, Chen et al. fabricated porous carbon derived from RHs, which showed a high capacitance of 368 $F g^{-1}$ at scan rate of 2 $mV s^{-1}$ [9]. However, the detailed supercapacitive properties such as rate performance and long-term cycle life of the carbon materials derived from RHs have not been investigated, which is very important for the application of RHs in electrochemical energy storage. Thus it is the motivation of the work presented here, and this approach can also be applied to other biomasses.

In this work, the nanoporous carbon was produced from RHs by first carbonizing at 550°C for 4 h, which was then followed by alkali hydroxide activation at 800°C. The nanoporous carbon has the average pore size of 2.2 nm and high specific area of 2523.4 $m^2 g^{-1}$. The specific capacitance

of the nanoporous carbon is calculated to be 250 F g^{-1} at the current density of 1 A g^{-1} and remains 198 F g^{-1} (about 80% of 250 F g^{-1}) when current density increased to 20 times (at the current density of 20 A g^{-1}), indicating excellent rate performance. The nanoporous carbon electrode from RHs also exhibits good long-term cycle life and the capacitance remains more than 90% after the first ~100 cycles and keeps stable till 10,000 cycles. The high capacitance, good rate performance, and long-term cycle life of the nanoporous carbon from RHs suggest the promising applications as SC electrode.

2. Experiments

2.1. Sample Preparation. All the chemicals are of analytical reagent and without further purification. RHs obtained from a local rice mill were firstly washed thoroughly with distilled water to remove soil and then boiled with HCl solution (2 mol L^{-1}) for 2 hours to get rid of the metallic oxide within RHs. The HCl treated RHs were annealed in a tube furnace at 550°C for 4 hours under N_2 to remove small organic molecules. After that, the precarbonized carbon was mixed with KOH with the mass ratio of 4 : 1 and further heated to 800°C for 1 hour under N_2. The product was washed with water for several times and then dried at 100°C. Finally, nanoporous activated carbon was produced. For comparison, the nonporous carbon was prepared with the similar procedures but without KOH activation during the heating process.

2.2. Sample Characterization. The samples were characterized by SEM (FE-SEM, FEI Nova Nano SEM 450), X-ray diffraction (XRD, Philips X' Pert Pro) with Cu Kα radiation of wavelength of 0.15416 nm at the range of 10~90°. The specific surface area of the sample was measured by the Brunauer-Emmett-Teller (BET) method with an automated chemisorption/physisorption surface area analyzer (Micromeritics ASAP 2020) at 77 K. The single point total pore volume was obtained from the amount of nitrogen adsorbed at a relative pressure around 0.97. The pore size distribution was derived from the adsorption branches of the isotherms by the density functional theory (DFT) method. FT-IR spectrum was tested by Perkin Elmer 1600.

2.3. Electrode Preparation and Electrochemical Evaluation. The nanoporous carbon from RH and polytetrafluoroethylene (PTFE) binder with the mass ratio of 9 : 1 were mixed thoroughly with ethanol as dispersant. The electrode film was fabricated by the doctor-blade technique on Ni foam with the area of about 1 × 1 cm^2. The loading amount of the active material was about 3.5 mg cm^{-2}. Electrochemical properties of nanoporous and nonporous carbon were measured based on three-electrode method using a CHI 660C instrument. The carbon coated on Ni foam (1 × 1 cm^2) acted as working electrode, a saturated calomel electrode (SCE) as the reference electrode, and a 2 × 2 cm^2 platinum plate as the counter electrode. KOH solution (6 M) served as the electrolyte. The cyclic voltammetry (CV) was performed from −1 to −0.2 V (*versus* SCE) at different scan rates (10–500 mV s^{-1}). The electrochemical impedance spectroscopy (EIS) data was tested at the open circuit potential (OCP). Galvanostatic charge/discharge curves were measured at different current densities over the potential range between −1 and −0.2 V (*versus* SCE). Cycling stability performance was conducted with a charge/discharge tester (Land CT2001A, Wuhan LAND Electronics Co., Ltd., China).

3. Results and Discussion

Figure 1 shows the FE-SEM images of the nonporous carbon (a) and nanoporous carbon (b), which illustrates that the sample activated by KOH has rough surface, while the sample without KOH activated has a massive appearance with a smooth surface. The wrinkle structure shown in Figure 1(b) indicates that the nanoporous carbon may have a high specific surface area which should be beneficial for ion adsorption, resulting in high specific capacitance. In order to investigate the nanoporosity of the carbon after KOH activation, N_2 adsorption-desorption isotherms and the corresponding pore size distribution were investigated. The BET adsorption and desorption isotherms of N_2 measured at 77 K on nonporous and nanoporous carbon are shown in Figure 2(a). The nanoporous carbon displayed type I desorption isotherm [10]; the amount of N_2 adsorbed was found to increase rapidly before relative pressure achieves 0.4 and then slow down after a relative pressure higher than 0.4 due to the nanoporous holes induced capillary condensation, meaning the carbon activated with KOH is microporous structure, while the isotherm for nonporous carbon has no characteristic of microporous structure. The nanoporous carbon indicates a high specific surface area of 2523.4 m^2 g^{-1} and a narrow pore size distribution centered at 2.2 nm (Figure 2(b)). The pore volume is as high as 1.36 cm^3 g^{-1}, suggesting potential application as high performance electrode for SCs.

XRD patterns of the nonporous carbon and the nanoporous carbon are shown in Figure 3. The diffraction patterns show broad but weak (002) reflection, indicating their disordered nature. The (002) reflection and a weak (100) reflection located at 43° suggest small islands of coherent and parallel stacked graphene sheets. Further FT-IR spectrum investigation shown in Figure 4 indicates the presence of carboxylic and hydroxyl groups located at 1560 and 3254 cm^{-1} band, respectively, which are reported to be able to produce extra pseudocapacitance for carbon materials [11, 12]. A high degree of turbostratic stacking of hexagonal graphene layers and the rich carboxylic and hydroxyl groups at the surface make the nanoporous C have excellent supercapacitive properties as in the detailed discussion in the following part.

The electrochemical impedance spectroscopy (EIS) was investigated to understand the resistance of the electrode assembled by the nonporous carbon and nanoporous carbon from RH, as shown in Figure 5. The nonporous carbon electrode without activating with KOH has the resistance of 1.7 ohm, and the nanoporous carbon electrode activated by

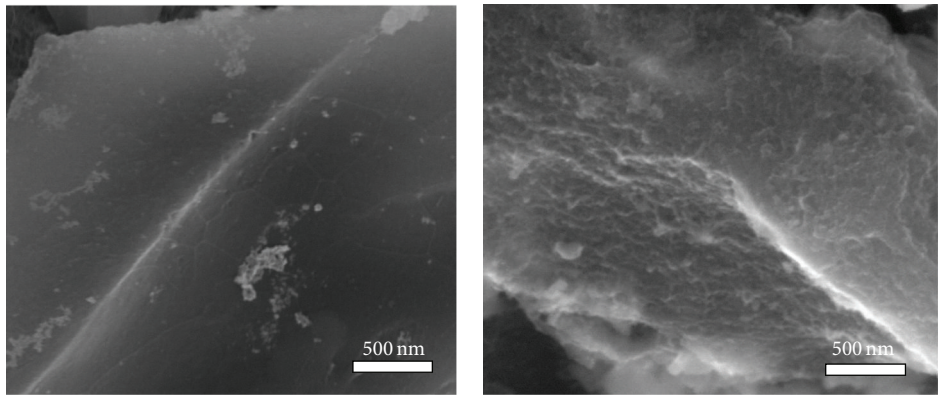

(a) (b)

Figure 1: FE-SEM images for the nonporous carbon (a) and the nanoporous carbon (b).

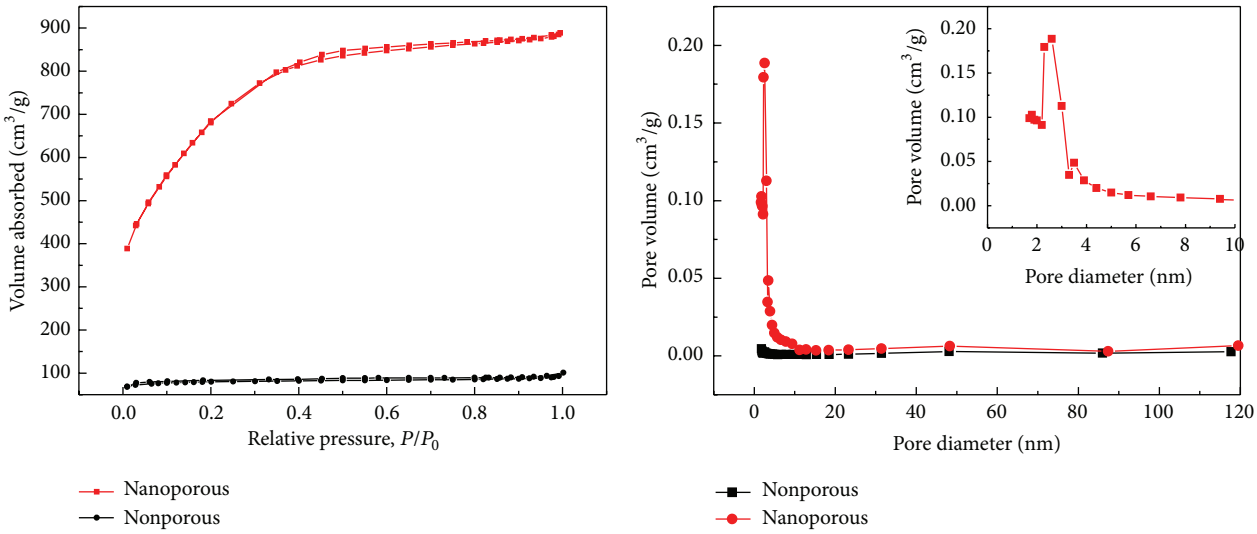

(a) (b)

Figure 2: (a) Adsorption and desorption isotherms of N_2 measured at 77 K on nonporous and nanoporous carbon. (b) Pore-size distribution profiles for the nonporous carbon and the nanoporous carbon. The inset is the enlarged view of nanoporous carbon in the pore diameter range of 0~10 nm.

KOH has a similar resistance of 1.3 ohm from the Nyquist plot, suggesting that the nanoporous carbon will have outstanding rate performance.

CV was performed to study the electrochemical properties of the nanoporous carbon electrode in 6 M KOH solution. As displayed in Figure 6(a), CV curves with scan rate of 10 mV s^{-1} of nonporous carbon and nanoporous carbon are markedly different. The area of CV curve of the nanoporous carbon electrode is much bigger than the nonporous carbon electrode indicating much higher capacity due to the nanoporosity and larger specific surface area produced from the activating process of KOH [13]. The CV curve of nanoporous carbon electrode exhibits a rectangular shape which is typical electric double-layer capacitance like other carbon material electrodes such as carbon nanotube and graphene [14, 15]. The deviation from rectangle at the bottom of two CV curves may attribute to ion-sieving effects caused by ultrafine pores which are not accessible in the N_2 adsorption [5, 16]. Figure 6(b) shows the charge/discharge curves with the current density of 1 A g^{-1} of nonporous carbon and nanoporous carbon electrodes. The capacitance of nanoporous carbon reaches 250 F g^{-1}, while the nonporous carbon only has the capacitance of 25 F g^{-1}. The nanoporous carbon activated by KOH shows the specific capacitance improved by ~10 times compared with nonporous carbon and the high capacitance of nanoporous C could be attributed to high specific area, large pore volume, and nanoporous structures, resulting in rich ion adsorption. Figure 6(c) shows the CV curves of nanoporous carbon electrode measured at scan rates of 10, 20, 50, 100, 200, and 500 mV s^{-1}, respectively. All the CV curves performed similar shape of rectangle even at a high scan rate of 200 mV s^{-1}, resulting from the high

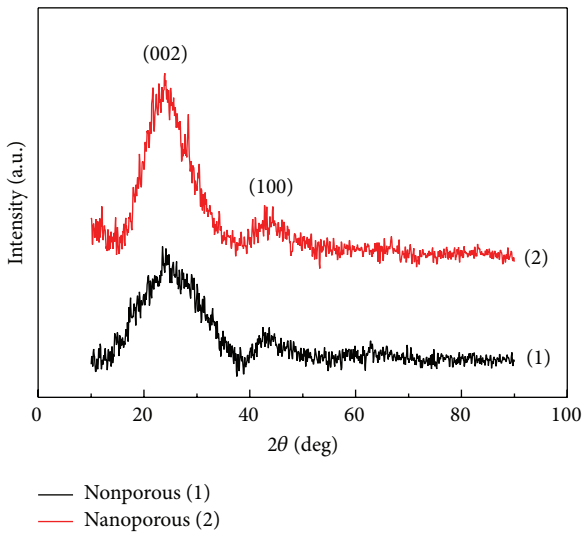

FIGURE 3: XRD patterns for the nonporous carbon (1) and the nanoporous carbon (2).

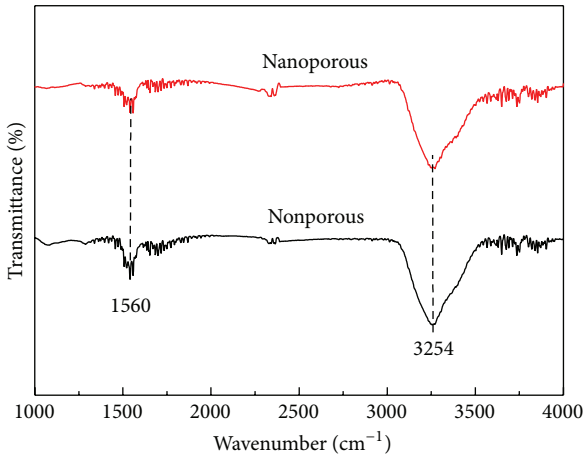

FIGURE 4: FT-IR spectrum of the nonporous carbon and nanoporous carbon.

conductivity and stable porous structure of the nanoporous carbon. The charge/discharge curves with the potential range of −1~−0.2 V (*versus* SCE) of the nanoporous carbon under current densities of 1, 2, 5, 10, 15, and 20 A g^{-1} are shown in Figure 6(d). The specific capacitance of the nanoporous carbon should be calculated according to the formula as follows [17]:

$$C_m = \frac{C}{m} = \frac{I \times \Delta t}{m \times \Delta V}, \quad (1)$$

where C_m (F g^{-1}) is the specific capacitance, I (A) is charge/discharge current density, Δt (s) is the discharge time, ΔV (V) is the potential range, and m (g) denotes weight of the active material on the electrode. The specific capacitance of nanoporous carbon was calculated to be 250, 239, 226, 214, 206, and 198 F g^{-1} at a current densities of 1, 2, 5, 10, 15, and 20 A g^{-1}, respectively, as shown in Figure 6(e). From

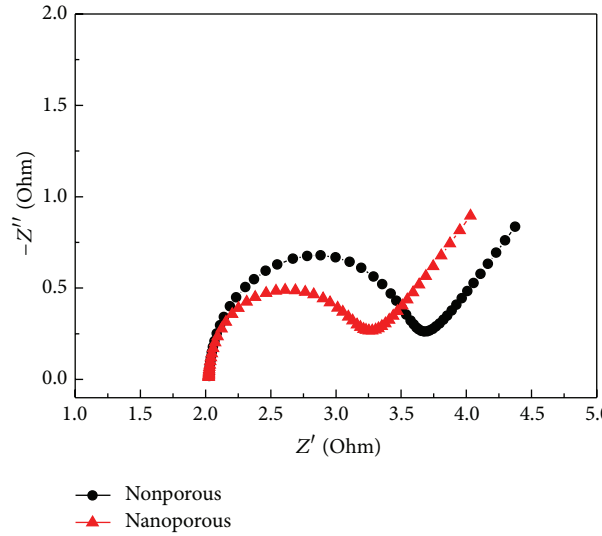

FIGURE 5: Nyquist plot of the nonporous carbon and the nanoporous carbon at the OCP in 6 M KOH solution.

the results, the specific capacitance of nanoporous carbon is much higher than that of nonporous carbon because of the porous structure and large specific surface area of the nanoporous carbon. The specific capacitance is higher than most of carbon based materials such as active carbon, CNT, or graphene [18–21]. In addition, it should be noted that the specific capacitance of nanoporous carbon still retains about 80% when the current density increases even up to 20 times (at 20 A g^{-1}), compared to the specific capacitance measured at 1 A g^{-1}. The high specific capacitance and excellent rate capability result from high conductivity and stable porous structure of nanoporous carbon.

For the electrochemical SCs, the two most important parameters are energy density and power density which are calculated from the following equations:

$$E = \frac{1}{2}CV^2,$$
$$P = \frac{E}{\Delta t}, \quad (2)$$

where P (W kg^{-1}) is the power density, C (F kg^{-1}) is specific capacitance, ΔV (V) is potential range, Δt (h) is discharge time, and E (Wh kg^{-1}) is the energy density. In terms of power density and energy density, our result (Figure 6(f)) shows that, at a power density of 0.4 kW kg^{-1}, an energy density of 22.2 Wh kg^{-1} can be obtained. When the power density is increased to 8 kW kg^{-1}, an energy density of 17.6 Wh kg^{-1} can be retained. These results indicate that the nanoporous carbon electrode could act as an excellent candidate that provides high power density with little loss in energy density for SCs.

Long-term cycle life performance is another important issue for SC. Cycling test of nanoporous carbon electrode was carried out at a current density of 1 A g^{-1} in 6 M KOH solution with the potential range between −1 and −0.2 V (*versus* SCE).

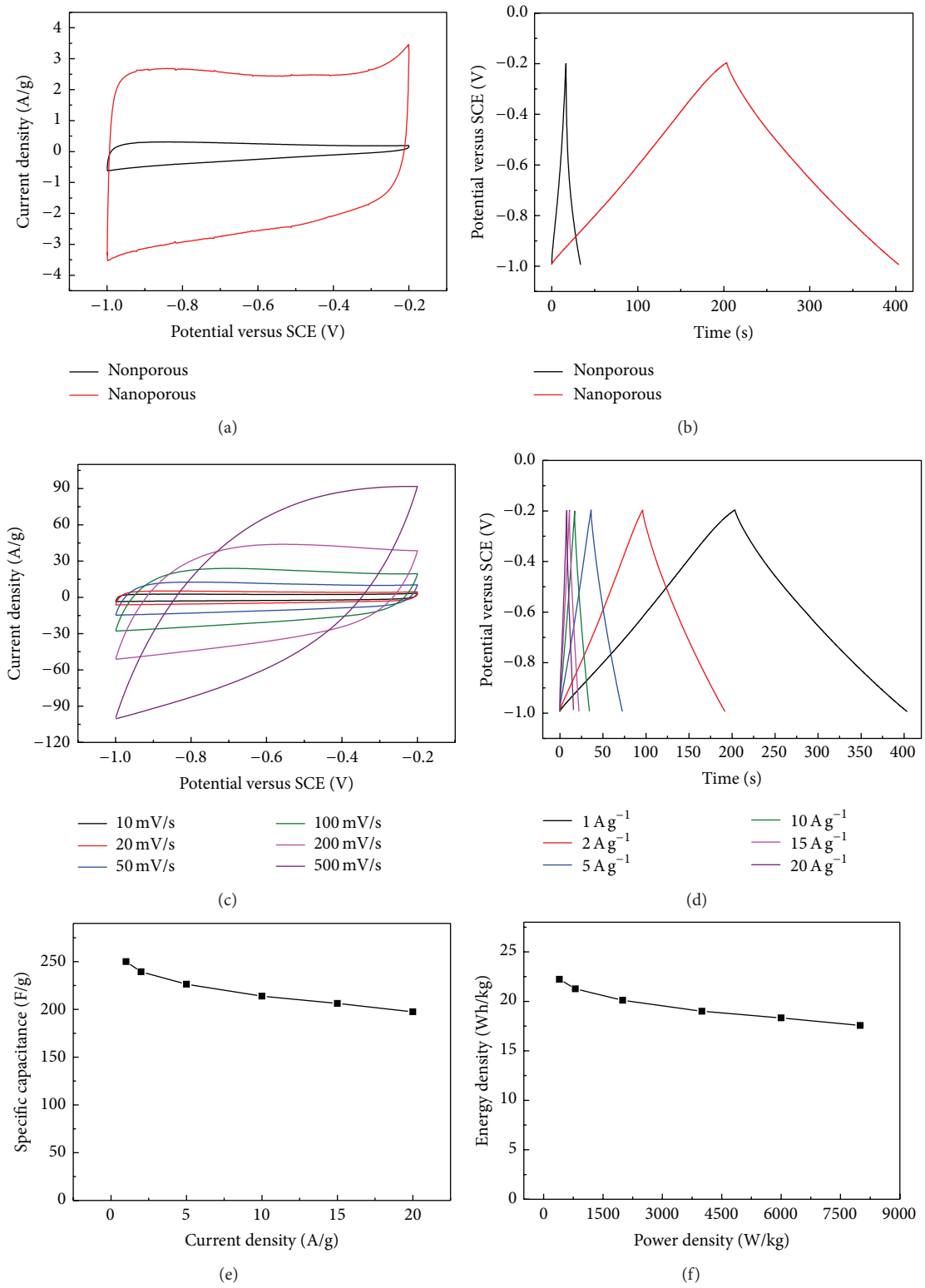

FIGURE 6: CV (a) and charge/discharge (b) curves for nonporous carbon and nanoporous carbon at the scan rate of 10 mV s^{-1} and current density of 1 A g^{-1}. (c) CV curves of the nanoporous carbon with different scan rate of 10, 20, 50, 100, 200, and 500 mV s^{-1}, respectively. (d) Charge/discharge curves of the nanoporous carbon with different current density of 1, 2, 5, 10, 15, and 20 A g^{-1}, respectively. (e) Rate performance of the nanoporous carbon electrode. (f) The relationship between energy density and power density for the nanoporous carbon. The electrolyte is 6 M KOH solution.

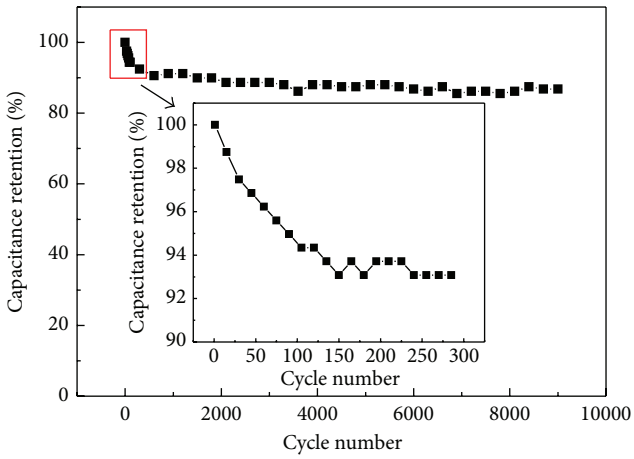

Figure 7: Cycle life performance for the nanoporous carbon of 10,000 cycles in the electrolyte of 6 M KOH solution at the current density of 1 A g^{-1}. The inset is the first 300 cycles of 10,000 cycles.

The curve of capacitance changes with the cycle number is shown in Figure 7. In the beginning ~100 cycles, the capacitance decreased ~8% and became quite stable after that till 10,000 cycles. This decreased capacitance in the first 100 cycles results from the removal of carboxylic and hydroxyl groups within the nanoporous structure and the disappearance of pseudocapacitance produced by these functional groups [22]. The high specific capacitance, excellent rate performance, and good cycle stability as well as low cost and facile preparation method indicate that the nanoporous carbon is an excellent electrode material for SCs.

4. Conclusions

The nanoporous activated carbon with large specific area of 2523.4 m^2 g^{-1} was obtained from RHs by precarbonizing at 550°C and activating with KOH at 800°C. It contains the average pore volume of 1.36 cm^3 g^{-1} and pore size of 2.2 nm. The as-prepared nanoporous carbon performs high specific of 250 F g^{-1} at the current density of 1 A g^{-1} in 6 M KOH solution electrolyte. Moreover, it also has an attractive rate performance that the specific capacitance remains 80% (198 F g^{-1}) at the current density of 20 A g^{-1} compared to the low current density of 1 A g^{-1} (250 F g^{-1}). The nanoporous activated carbon electrode also expresses amazing long-term cycle life performance that it maintains more than 90% after the first ~300 cycles and then keeps stable till 10,000 cycles. The superior capacitive performance and the low cost and facile fabrication method of the nanoporous activated carbon electrode make it a very promising candidate for SCs applications.

Conflict of Interests

The authors declare that there is no conflict of interests regarding the publication of this paper.

Acknowledgments

This work was financially supported by the National Natural Science Foundation of China (Grants nos. 50902104 and 21105077), the Outstanding Young and Middle-Aged Scientific Innovation Team of Colleges and Universities of Hubei Province (T201402), and the Applied Basic Research Program of Wuhan City (2013011801010598).

References

[1] H. Jiang, P. S. Lee, and C. Li, "3D carbon based nanostructures for advanced supercapacitors," *Energy and Environmental Science*, vol. 6, no. 1, pp. 41–53, 2013.

[2] M. Zhi, C. Xiang, J. Li, M. Li, and N. Wu, "Nanostructured carbon-metal oxide composite electrodes for supercapacitors: a review," *Nanoscale*, vol. 5, no. 1, pp. 72–88, 2013.

[3] L. Qie, W. Chen, H. Xu et al., "Synthesis of functionalized 3D hierarchical porous carbon for high-performance supercapacitors," *Energy & Environmental Science*, vol. 6, no. 8, pp. 2497–2504, 2013.

[4] X. Hong, K. S. Hui, Z. Zeng et al., "Hierarchical nitrogen-doped porous carbon with high surface area derived from endothelium corneum gigeriae galli for high-performance supercapacitor," *Electrochimica Acta*, vol. 130, pp. 464–469, 2014.

[5] Z. Li, L. Zhang, B. S. Amirkhiz et al., "Carbonized chicken eggshell membranes with 3D architectures as high-performance electrode materials for supercapacitors," *Advanced Energy Materials*, vol. 2, no. 4, pp. 431–437, 2012.

[6] A. Elmouwahidi, Z. Zapata-Benabithe, F. Carrasco-Marín, and C. Moreno-Castilla, "Activated carbons from KOH-activation of argan (*Argania spinosa*) seed shells as supercapacitor electrodes," *Bioresource Technology*, vol. 111, pp. 185–190, 2012.

[7] Y. Ren, J. Zhang, Q. Xu et al., "Biomass-derived three-dimensional porous N-doped carbonaceous aerogel for efficient supercapacitor electrodes," *RSC Advances*, vol. 4, no. 45, pp. 23412–23419, 2014.

[8] A. Salanti, L. Zoia, M. Orlandi, F. Zanini, and G. Elegir, "Structural characterization and antioxidant activity evaluation of lignins from rice husk," *Journal of Agricultural and Food Chemistry*, vol. 58, no. 18, pp. 10049–10055, 2010.

[9] H. Chen, H. Wang, L. Yang et al., "High specific surface area rice hull based porous carbon prepared for EDLCs," *International Journal of Electrochemical Science*, vol. 7, no. 6, pp. 4889–4897, 2012.

[10] K. S. W. Sing, D. H. Everett, R. A. W. Haul et al., "Reporting physisorption data for gas/solid systems-with special reference to the determination of surface area and porosity," *Pure and Applied Chemistry*, vol. 57, pp. 603–619, 1985.

[11] U. J. Kim, C. A. Furtado, X. Liu, G. Chen, and P. C. Eklund, "Raman and IR spectroscopy of chemically processed single-walled carbon nanotubes," *Journal of the American Chemical Society*, vol. 127, no. 44, pp. 15437–15445, 2005.

[12] M. Seredych, D. Hulicova-Jurcakova, G. Q. Lu, and T. J. Bandosz, "Surface functional groups of carbons and the effects of their chemical character, density and accessibility to ions on electrochemical performance," *Carbon*, vol. 46, no. 11, pp. 1475–1488, 2008.

[13] J. Wang and S. Kaskel, "KOH activation of carbon-based materials for energy storage," *Journal of Materials Chemistry*, vol. 22, no. 45, pp. 23710–23725, 2012.

[14] P. Simon and Y. Gogotsi, "Materials for electrochemical capacitors," *Nature Materials*, vol. 7, no. 11, pp. 845–854, 2008.

[15] Y. Wang, Z. Shi, Y. Huang et al., "Supercapacitor devices based on graphene materials," *The Journal of Physical Chemistry C*, vol. 113, no. 30, pp. 13103–13107, 2009.

[16] L. Eliad, G. Salitra, A. Soffer, and D. Aurbach, "Ion sieving effects in the electrical double layer of porous carbon electrodes: Estimating effective ion size in electrolytic solutions," *The Journal of Physical Chemistry B*, vol. 105, no. 29, pp. 6880–6887, 2001.

[17] C.-C. Hu and C.-C. Wang, "Improving the utilization of ruthenium oxide within thick carbon-ruthenium oxide composites by annealing and anodizing for electrochemical supercapacitors," *Electrochemistry Communications*, vol. 4, no. 7, pp. 554–559, 2002.

[18] E. O. Fedorovskaya, L. G. Bulusheva, A. G. Kurenya, I. P. Asanova, and N. A. Rudina, "Supercapacitor performance of vertically aligned multiwall carbon nanotubes produced by aerosol-assisted CCVD method," *Electrochimica Acta*, vol. 139, pp. 165–172, 2014.

[19] T. Kim, G. Jung, S. Yoo, K. S. Suh, and R. S. Ruoff, "Activated graphene-based carbons as supercapacitor electrodes with macro- and mesopores," *ACS Nano*, vol. 7, no. 8, pp. 6899–6905, 2013.

[20] B. Zheng, T.-W. Chen, F.-N. Xiao, W.-J. Bao, and X.-H. Xia, "KOH-activated nitrogen-doped graphene by means of thermal annealing for supercapacitor," *Journal of Solid State Electrochemistry*, vol. 17, no. 7, pp. 1809–1814, 2013.

[21] E. G. Calvo, F. Lufrano, P. Staiti, A. Brigandì, A. Arenillas, and J. A. Menéndez, "Optimizing the electrochemical performance of aqueous symmetric supercapacitors based on an activated carbon xerogel," *Journal of Power Sources*, vol. 241, pp. 776–782, 2013.

[22] Y. Bai, R. B. Rakhi, W. Chen, and H. N. Alshareef, "Effect of pH-induced chemical modification of hydrothermally reduced graphene oxide on supercapacitor performance," *Journal of Power Sources*, vol. 233, pp. 313–319, 2013.